Article

Not peer-reviewed version

Modelling and Simulation of Wind Farm Integrated with Grid Utilizing Doubly Fed Induction Generator

Moula Bux Kanhio * and Farhat Naureen Memon

Posted Date: 12 March 2025

doi: 10.20944/preprints202503.0844.v1

Keywords: Renewable energy resources; Wind variable speed; Wind farm; DFIG

Article

Modelling and Simulation of Wind Farm Integrated with Grid Utilizing Doubly Fed Induction Generator

Moula Bux Kanhio * and Farhat Naureen Memon

Institute of Mathematics & Computer Science, University of Sindh, Jamshoro Pakistan
* Correspondence: mbkanhio@gmail.com

Abstract: At present, Due to a scarcity of power, Pakistan is facing major load shedding and blackout issues. In order to address this issue, renewable energy resources (RESs) may be a suitable option. Pakistan is blessed with many RESs such as solar, wind and hydro. The present energy crisis may be solved suitably if the Pakistan generates electrical power from these RESs. Among these RESs, wind energy is preferable because it is cost-effective and environmentally friendly. Power generated from wind farm can be integrated with grid through voltage source converter (VSC) in order to meet increased load demand. Wind farms commonly use different types of generators; doubly fed induction generator (DFIG) based wind variable speed technology is presently the most often utilized in wind farms, due to its many benefits. This study based on modelling and simulation of 9 MW wind farm based on DFIG using MATLAB/Simulink software version 2020a. The designed wind farm will be integrated with Grid and its performance will be analyzed for various wind speed variation cases in order to show its effectiveness.

Keywords: renewable energy resources; wind variable speed; wind farm; DFIG

---

1. Introduction

Energy has been magnificent resource and critical requirement for advancement of human technology. The size of power producing systems has increased to keep up with the 21st century's rising demand for electricity. Global energy scarcity is a result of urbanization and rapid population expansion. Power generation systems can be divided into two main types based on their exhaustibility: conventional energy systems and non-conventional energy systems. Conventional energy comes from limited sources like nuclear fuels and fossil fuels (coal, crude oil, and natural gas) and non- conventional energy comes from natural resources like solar, biogas, wind, water stream, geothermal energy, and tidal energy [1].

It is essential to enhance electrical energy output through RESs including wind, solar, and other energy sources due to rise in electrical energy demand and decline in traditional energy sources[1–6]. Worldwide, steam power plants account for a sizeable portion of the per-capita production of electricity, which is still mostly produced using fossil fuels like coal and gas. Thus, fossil fuel-based power systems serve as the main energy source and are constantly looking for ways to enhance in a variety of areas, including environmental factors [7], controllability, stability, and dependability. The utility and end user's rising energy bills are partly caused by inadequate quality control and expensive maintenance costs. Additionally, there are finite supplies of fossil fuels like coal, gas, and petroleum, and they cause dangerous air pollution [8]. Furthermore, hazardous radioactive waste from nuclear power plants is produced, such as plutonium isotopes, which pose a health risk to people and other living things, including livestock. Furthermore, compared to other power plants, nuclear power plants require significantly higher maintenance costs [9]. Fossil fuels are scarce and will eventually run out, in addition to the hazardous wastes, environmental problems, high operating costs as well as maintenance issues.

 doi:10.20944/preprints202503.0844.v1

Thankfully, RESs like wind, solar, geothermal, tidal, and fuel cells [10,11] have been bestowed upon us by nature. These sources are prevalent in rural areas and will always exist. Because it produces no emissions, wind energy is still a popular and environmentally friendly option when it comes to renewable energy that comes from natural sources [12].

Due to its lower manufacturing, installation, and design complexity, developing nations can readily adopt wind energy conversion systems (WECS), which are electrical power generation source with the fastest rate of growth in the world and will account for a large portion of world's electricity capacity in the future.

The kinetic wind power that strike rotor blades of wind turbine transformed into mechanical rotational energy [13]. Depending on the rotor speed, wind turbines are divided into two categories: fixed speed wind turbines (FSWT) and variable speed wind turbines (VSWT). Regardless of wind speed, the spinning speed with FSWT technology stays constant. The VSWT may modify its rotor speed in response to abrupt variations in wind speed. VSWTs are typically more interesting than fixed-speed turbines when wind speed fluctuates significantly. Several factors, such as reduced mechanical part stress, reduced acoustic noise, and enhanced power quality, make VSWT superior to WECS's erratic running speed.

DFIG-based WECS are popular and widely utilized worldwide. These systems replace slip ring induction motors or wound rotor induction machines with DFIGs, which are electrical power conversion devices. The power and speed of the rotor can be changed thanks to electrical converters. Because it allows electrical energy to flow both ways—into the rotor when the generator is operating at sub-synchronous speed and into the grid when it is operating at super-synchronous speed—the stator of a wound rotor induction machine is directly connected to the grid, while the rotor windings are connected to the grid through back-to-back converters. This arrangement is known as DFIG. The rotor circuit and grid are connected via a bidirectional AC/DC/AC converter, which controls speed above synchronous. Power is produced by the rotor and stator [9].

The following are the primary benefits of DFIG [14]:

Able to supply power at a constant frequency and voltage even when the rotor speed fluctuates.

By adapting the rotor speed to the wind speed, wind generator efficiency can be increased.

Power electronic converters require lower power ratings because they only need to control a part of the total power.

Reactive and active power can be individually controlled, allowing power factor to be controlled [15].

The generator and transformer supply the grid with the primary electricity that exits the stator. About 30% rated power amount back-to-back converter can handle in terms of power. As a bisectional power flow, this back-to-back converter operates. First, rotor side converter (RSC) converts rotor power to DC [16] then grid side converter (GSC) used to convert DC to AC once more and fed to grid via the transformer. These converters preserve the grid line and protect the machine from damage when wind speeds vary [17]. The exchange of reactive and active power to grid is handled by RSC. By using reactive power exchange, GSC controls grid point of common coupling power factor and DC link voltage [18].

This study focuses; the designed wind farm (9 MW) will be integrated with Grid through VSC and its performance will be analyzed for various wind speed variation cases in order to show its effectiveness. This will help in installing the Wind Turbine with DFIG in hardware at the wind area.

1.1. Main Objectives & Contribution

The article explains the potential of wind energy and how to harness it to produce additional electrical energy. The significance and operation of DFIG linked with wind turbine are also highlighted in this research. Following are the main objectives of the research:

To design model of 9 MW wind farm based DFIG in MATLAB/SIMULINK version 2020a.

To design a grid model in MATLAB/SIMULINK version 2020a and integrate it with wind farm.

 doi:10.20944/preprints202503.0844.v1

To design a model of Voltage Source Converter (AC-DC and DC-AC conversion).
A model of 9 MW wind farm will be integrated with grid.
Analyze the performance of grid connected wind farm for various wind speed variation cases.

1.2. Structure of the Article

The following is the arrangement of the manuscript: Section 1 explains the significance of using wind energy conversion system (WECS) based on DFIG. Section 2 provides an overview of the literature in WECS technology. Section 3 Provides the grid-connected DFIG-based WECS system structure and wind farm modeling. Section 4 provides the analysis of simulation and simulation outcomes for the suggested system using variable input wind speed. Finally, we conclude up the proposed study with future work in section 5.

2. Literature Review

The literature review on the state-of-the-art in WECS covered in this section. It is founded on the division of wind turbine-based generating systems into two main categories: FSWTs and VSWTs. When it came to wind turbine generators (WTGs) with FSWTs, the squirrel cage induction generator (SCIG) was the most widely utilized type of generator in the past. For the past few decades, the usage of isolated asynchronous generators (IAGs) for stand-alone power generation has shown promise because of its large torque/weight ratio, intrinsic short circuit protection, brushless construction, simplicity, and ease of maintenance. The biggest obstacles to IAG's commercial adoption are its inadequate frequency and voltage control capabilities. Moreover, when a load is directly connected across IAG bus, prime-mover speed which depends on input wind power and related consumer loads determines IAG frequency. In terms of frequency stability, reactive power compensation, and voltage control, VSC makes it easier to achieve improved system behavior. VSWTs are now employed in WECS innovation. Because electronics converters' power enables total decoupling from grid, variable speed activity is made possible. Based on its ability to increase wind energy harvesting capacity for a given machine rating in WECS, DFIG-based WECS has been recommended, as demonstrated by the obtained results [9]. The only machine that can deliver more power than it is rated for without overloading is the DFIG [19]. Consistent voltage and frequency of power can be supplied via DFIG even when prime mover speed changes. In addition, the DFIG lowers the controller rating overall and is controllable from the rotor side. In [20] have revealed that DFIG-based energy conversion system uses back-to-back coupled VSC, regulate system's active and reactive power while supplying generated power to the grid.

Figure 1 provides a summary of the many kinds of wind power generating technologies. A summary of the main categories for wind turbine generators is also given in Table 1, which includes information on gearboxes, soft starters, speed range, generator types, power voltage converters, aerodynamic power control, active power control, and reactive power compensation requirements.

Table 1. The primary distinctions among the various WECS configuration types.

Types of Wind Turbine Generators (WTGs)				
Wind turbine technology	**Fixed speed**	**Semi-variable speed**		**Full-variable speed**
Wind generator kinds	SCIG	Variable rotor resistance (WRIG)	DFIG	PMSG
Generator types	Kind 1	Kind 2	Kind 3	Kind 4
Power converters	No	Partial	Partial	Full
Speed range	Less than 1% rated	Less than 10% rated	±30% of ratings	complete, 100% rated
Soft starter	Yes	Yes	No	No

Preprints.org (www.preprints.org) | NOT PEER-REVIEWED | Posted: 12 March 2025 doi:10.20944/preprints202503.0844.v1

Gearbox	Yes	Yes	Yes	Optimal
Control of aerodynamic power	Pitch, Stall, Active stall	Pitch	Pitch	Pitch
Reactive power compensator on grid side	Yes	Yes	No	No
MPPT and active power control	N/A	Limited	Yes	Yes
Short circuit (fault active)	No	No	No/Yes	Yes
Efficiency rating	Low	Low/reduced	Good	Good

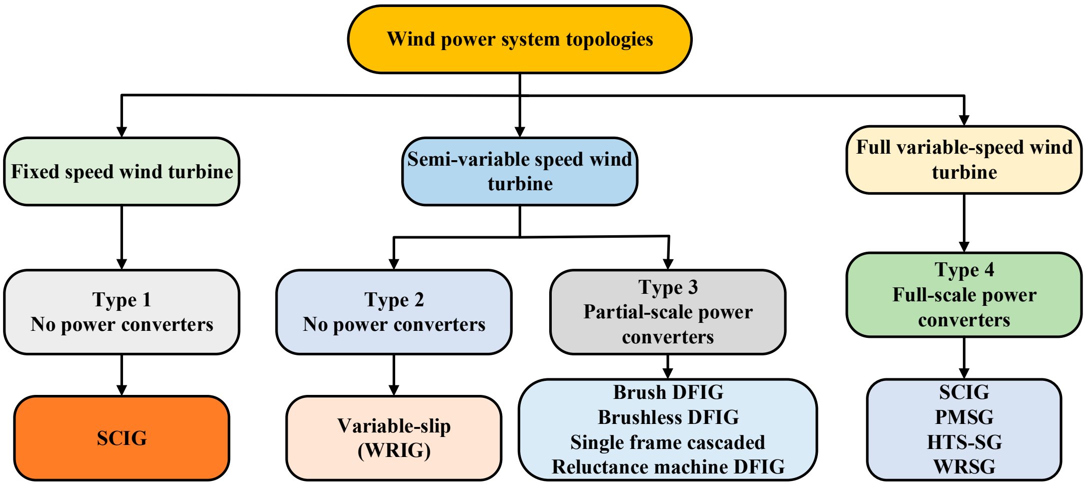

Figure 1. A summary of various types of wind energy generation systems.

3. Suggested DFIG System Framework and Modeling

Proposed system framework of grid-connected DFIG wind farm shown in Figure 2. Suggested framework allows for the delivery of 9 MW power. The system consists of a back-to-back three-phase pulse width modulated (PWM) VSC, DFIG, DC-link capacitor, and wind turbine. The VSC with the rotor winding connection is called the RSC. VSC connected at point of coupling (PoC) GSC, while stator winding is directly connected with grid [21]. Various working conditions of a DFIG are attained by RSC and GSC. The suggested system's active and reactive power flow diagram is displayed in Figure 3.

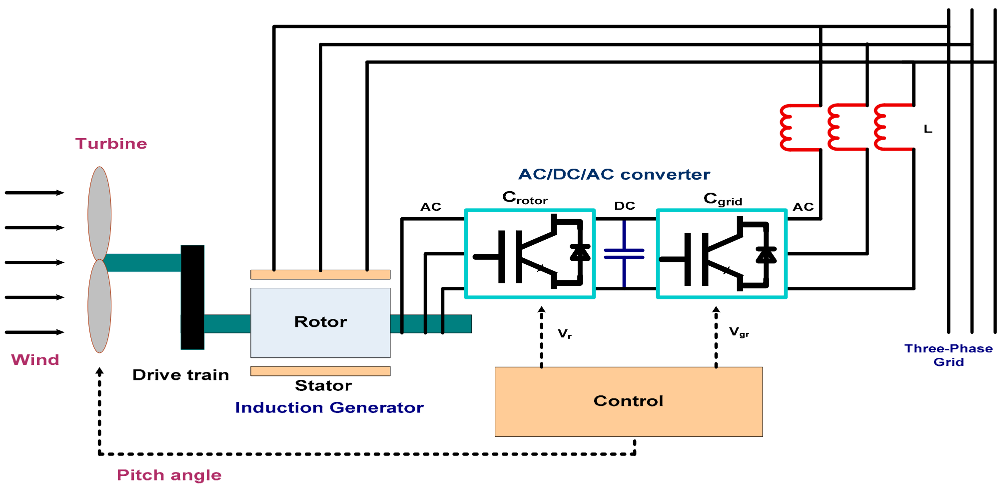

Figure 2. Wind turbine configuration with variable speed and DFIG.

 doi:10.20944/preprints202503.0844.v1

Where V_r represents rotor voltage and V_{gr} grid side voltage. Wind turbine-driven DFIG system's harmonics are reduced by AC/DC/AC converter, which is essentially PWM converter that applies sinusoidal PWM technology. C_{rotor} RSC and C_{grid} GSC.

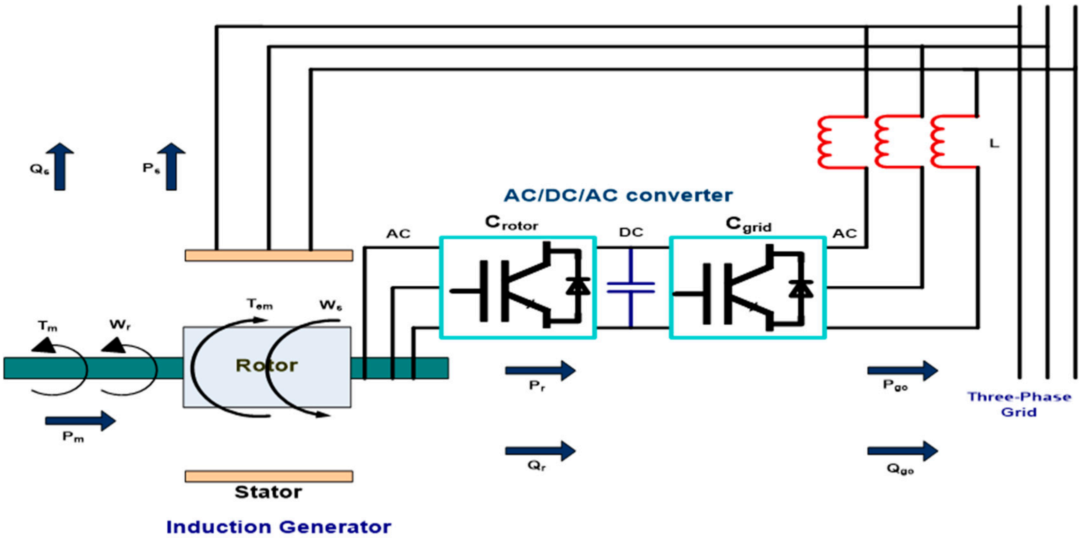

Figure 3. Power flow diagram of DFIG.

Where P_m wind turbine's mechanical power transferred to rotor P_s stator electrical power output, P_{gc} generation of electrical power (C_{gr}), Q_s output of stator reactive power, Q_r reactive power output of rotor, Q_{gc} reactive power output (C_{grid}), T_m torque exerted mechanically on rotor, T_{em} rotor experiences electromagnetic torque from generator., ω_r rotor rotating speed.

3.1. Modelling of Wind Turbine

Wind power is one of the primary unconventional energy sources. The wind power system integrates a wind turbine generator (WTG) with an existing power infrastructure [22]. The dynamic model of the WTG is as follows:

$$\Delta P_{WTG} = \frac{1}{T_{WTG}} \Delta P\omega - \frac{1}{T_{WTG}} \Delta P_{WTG} \quad (1)$$

T_{WTG} stands for WTG's time constant, P_ω for wind power, and ΔP_{WTG} for WTG's output power change. A turbine's rotor, which has blades, converts wind energy into mechanical energy. The following formulas provide a mathematical representation of the rotor's extracted wind power.[23].

$$P_{rotor} = \frac{1}{2} \rho A V^3 C_p \quad (2)$$

where A stands for sweeping area, V for wind speed (velocity), C_p for power coefficient, and ρ for wind density. The relationship between input wind speed and active power can be demonstrated using the following.

$$P_{GW} = \frac{\rho a^2 V_\omega^3 C_p}{2} (T_{SR}, \beta) \quad (3)$$

where V_ω wind speed and rotor efficacy C_p are expressed as follows, β represents the blade's angle, T_{SR} tip speed ratio, area density, and swept.

Preprints.org (www.preprints.org) | NOT PEER-REVIEWED | Posted: 12 March 2025 doi:10.20944/preprints202503.0844.v1

$$C_p = \frac{T_{SR} - 0.022\beta^2 - 5.6}{2} e^{-0.17 T_{SR}}$$
$$T_{SR} = \frac{r_{pm}\pi D}{60V} \tag{4}$$

Turbine generated torque expressed by:

$$T_t = \frac{P_{GW}}{\omega t} \tag{5}$$

While ωt represents the wind turbine rotor's angular rotational speed.

3.2. Modelling of DFIG

The DFIG consists of stator and rotor windings. The stator's three-phase insulated windings connect to the grid via a transformer, while the rotor, also with three-phase windings, links to an external circuit through slip rings and brushes. These components enable controlled current injection or absorption into the rotor windings [24–27].

Direct and inverse transformations serve as a representation of the DFIG's dynamic model. Rotor and stator's three windings can be described by two windings using space vector theory $\alpha\beta$ stationary for stator and winding dq rotating for rotor.

Voltage vectors for stator and rotor represented as:

$$\vec{u_s} \rightarrow \begin{Bmatrix} u_{ds} = R_s i_{ds} + \dfrac{d\psi_{ds}}{dt} - \omega_s \psi_{qs} \\ u_{qs} = R_s i_{qs} + \dfrac{d\psi_{qs}}{dt} - \omega_s \psi_{ds} \end{Bmatrix} \tag{6}$$

$$\vec{u_s} \rightarrow \begin{Bmatrix} u_{dr} = R_r i_{dr} + \dfrac{d\psi_{dr}}{dt} - \omega_r \psi_{qr} \\ u_{qr} = R_r i_{qr} + \dfrac{d\psi_{qr}}{dt} - \omega_r \psi_{dr} \end{Bmatrix} \tag{7}$$

where u_{ds}, u_{qs}, u_{dr} & u_{qr} represents stator and rotor voltages in dq frame. i_{ds}, i_{qs}, i_{dr} & i_{qr} represents stator and rotor current in dq frame. R_s, R_r, ω_s & ω_r represents stator and rotor phase resistances, and angular velocity.

Electromagnetic torque given as follows:

$$T_{em} = \frac{3}{2} p \frac{L_m}{L_s} (\psi_{qs} i_{dr} - \psi_{ds} i_{qr} \tag{8}$$

Following formulas provide stator and rotor's active and reactive power:

$$\begin{Bmatrix} P_S = \dfrac{3}{2}(u_{ds} i_{ds} + u_{qs} i_{qs} \\ Q_S = \dfrac{3}{2}(u_{qs} i_{ds} - u_{ds} i_{qs} \end{Bmatrix} \tag{9}$$

Preprints.org (www.preprints.org) | NOT PEER-REVIEWED | Posted: 12 March 2025 doi:10.20944/preprints202503.0844.v1

$$\begin{cases} P_r = \frac{3}{2}(u_{dr}i_{dr} + u_{qr}i_{qr} \\ Q_r = \frac{3}{2}(u_{qr}i_{dr} - u_{dr}i_{qr} \end{cases} \tag{10}$$

where P_s, Q_s indicate active and reactive power of stator. P_r, Qr shows rotor active and reactive power. T_{em} denotes electromagnetic torque. Fundamental torque expression is as follows:

$$T_{em} - T_{load} = J\frac{d\omega_m}{dt} \tag{11}$$

J represents inertia of rotor, T_{load} load torque applied on shaft and ω_m rotor speed.

3.3. Operational Features of DFIG Powered by Wind Turbine

DFIGs are a class of induction generators in wind turbines, featuring wound rotors and AC/DC/AC IGBT-based PWM inverters. The stator is directly linked to the 50 Hz grid, while the rotor functions at a variable frequency via the inverter. This technology enhances wind energy capture at low speeds and minimizes mechanical stress by regulating turbine speed during gusts. The ideal turbine speed, directly proportional to wind velocity, maximizes energy output. When wind speed is below 10 m/s, the rotor runs sub-synchronously, whereas at higher speeds, it operates hyper-synchronously. Unlike SCIGs, DFIGs eliminate the need for capacitor banks, as their converters can regulate reactive power.

Figure 4 illustrates the ABCD curve on the turbine's mechanical power profile at different wind speeds. The power control loop uses this characteristic to regulate turbine speed (ω_r). Defined by points A, B, C, and D, reference power is zero up to A, follows a tracking path from A to B, peaks between B and C, and forms a straight line from C to D, reaching 1 pu where it stabilizes. Table 2 details these points.

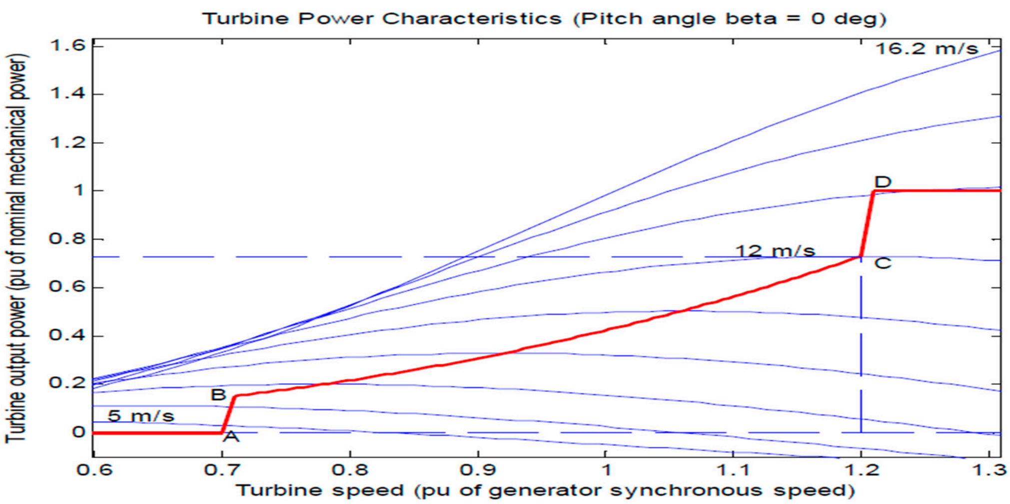

Figure 4. Turbine power characteristics.

Table 2. Statistics of point A, B, C and D.

Spot	Wind Velocity (m/s)	Speed of Turbine	Power Output of a Turbine (pu)
A	4.23	0.7	0
B	7.1	0.71	0.151
C	12	1.2	0.73

Preprints.org (www.preprints.org) | NOT PEER-REVIEWED | Posted: 12 March 2025 doi:10.20944/preprints202503.0844.v1

3.4. Single-Line Diagram of a Wind Farm Connected to a Distribution Network

A distribution network links to a 9 MW wind farm. A generator is incorporated into a compact power system and interfaced with an infinite bus through line impedance. The simplified system is shown in Figure 5.

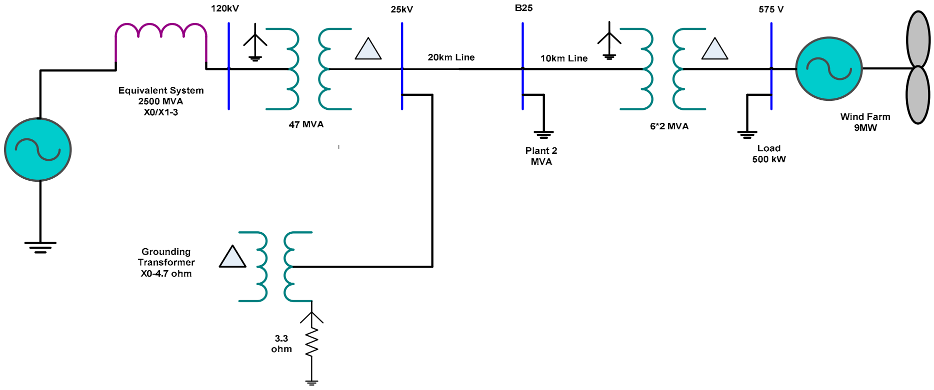

Figure 5. A single line schematic showing a wind farm linked to the distribution network.

Figure 5 shows a 9 MW wind farm with six 1.5 MW turbines connected to a 25 kV distribution system, delivering power via a 30 km, 25 kV feeder to a 120 kV grid. At bus B25, a 2 MVA, 2300 V plant is connected, featuring a 1.68 MW induction motor (0.93 PF) and a 200-kW resistive load. A 500-kW load is also connected to the wind farm's 575 V bus. This section covers the modeling of the 9 MW wind farm with grid integration, while Section 4 focuses on MATLAB/Simulation modeling to analyze the operation of the wind power plant with a DFIG system at varying wind speeds.

4. Simulation Results

MATLAB/Simulink environment used to implement and simulate suggested modeling. This section examines suggested system's performance in relation to variations in wind speed. Table 3 displays the parameters of the system's simulation.

Table 3. Simulation parameters for the model.

Specifications	Specifications Value
Air density	1.225 kg/m^3
Pitch angle	0^o
Nominal power	9MW
Frequency	50Hz
Rated torque	12732 N.m
Pole pair	2
Inertia	127 Kg.m^2
Gear ratio	100
Radius of turbine	42
Power factor	0.9
Dc bus capacitor	6×10^4 μF
Reference voltage	1 pu
Voltage droop	0.02 pu
Gain value	[1 exp(j×2×pi/3) exp(-j×2×pi/3)]

Figure 6 shows DFIG model in MATLAB/Simulink environment. Simulink modeling of wind turbine and grid data acquisition displayed in Figures 7 and 8.

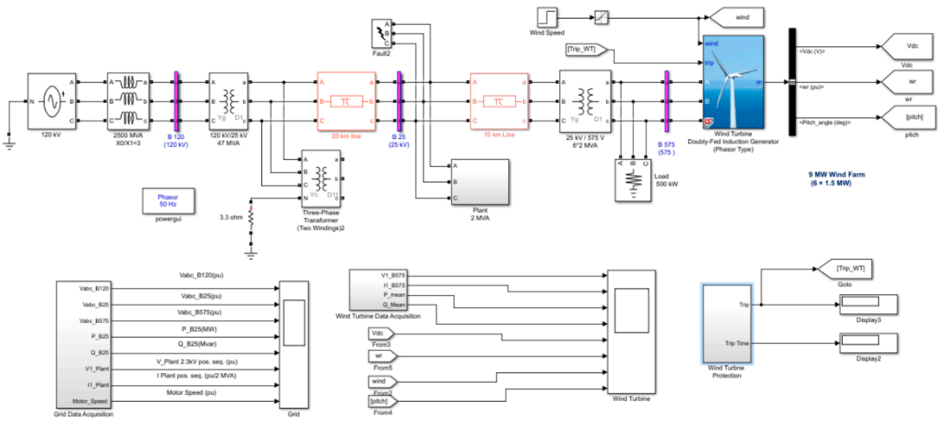

Figure 6. Grid-connected DFIG Simulink model.

The Simulink model for a DFIG connected to grid side displayed in Figure 6, along with wind turbine protection schemes that used to protect against ground faults and single-phase faults. A 9 MW wind farm (six of 1.5 MW each) connected with system via a 120 kV, three phase source, step down transformers, fault prevention, and pi transmission line.

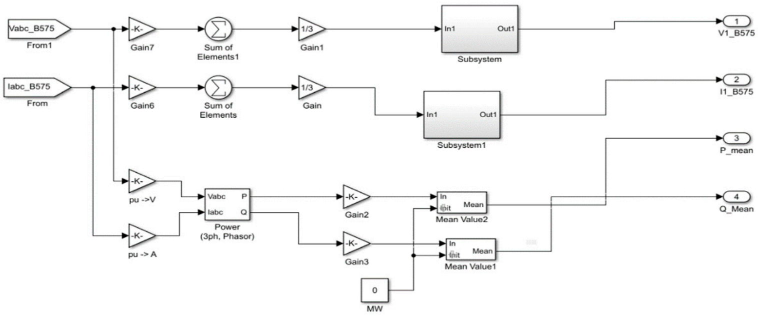

Figure 7. Acquisition of data from wind turbine.

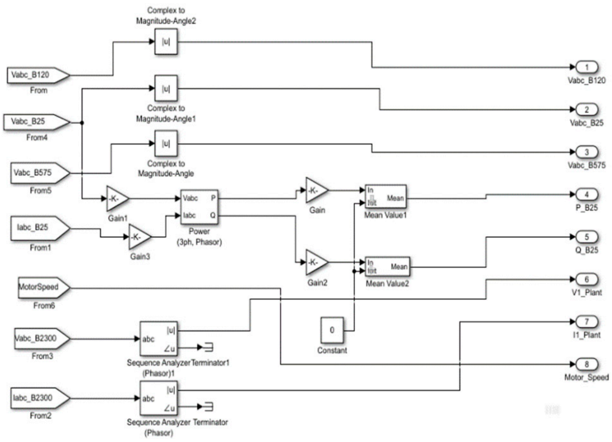

Figure 8. Acquisition of data from grid.

4.1. Turbine Response When Wind Speed Lower Than its Rated Value (Case 1)

Observe how turbine response when wind speed changes. As shown in Figure 9, wind speed initially set at 8 m/s and increases abruptly to 10 m/s at t = 5 seconds.

Preprints.org (www.preprints.org) | NOT PEER-REVIEWED | Posted: 12 March 2025 doi:10.20944/preprints202503.0844.v1

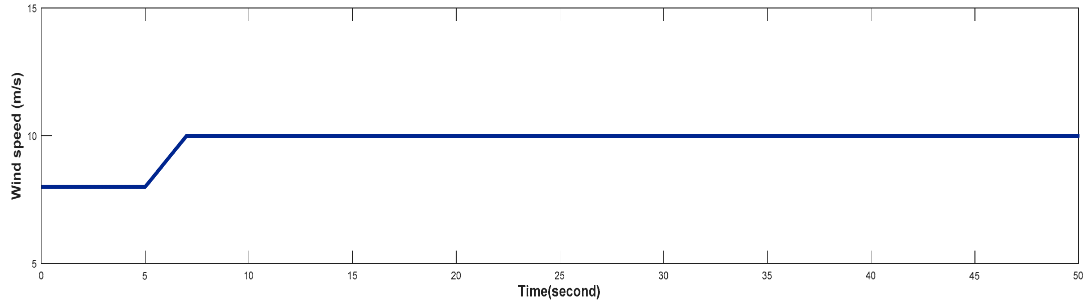

Figure 9. Wind speed changes from 8–10 m/s.

The rotor speed rises gradually as wind speed abruptly shifts from 8 to 10 m/s, and it eventually settles to 1pu, which is not its rated value, after a few milliseconds. Figure 10 depicts rotor speed (ω_r) behavior.

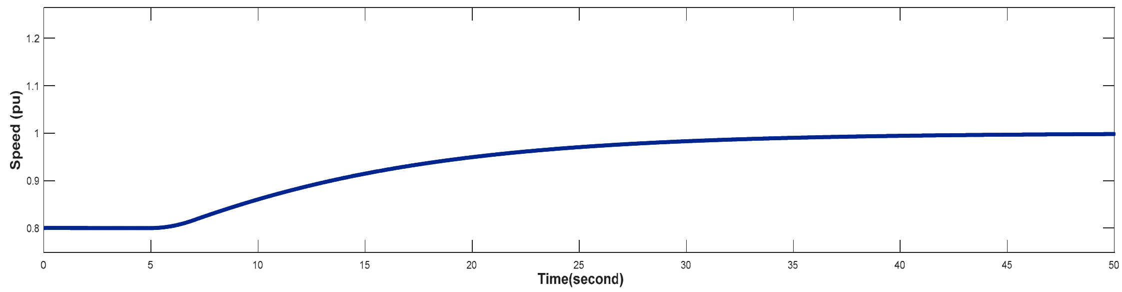

Figure 10. Rotor speed curve at wind speed 8–10 m/s.

As speed of wind changes, current changes and thus power generated changes. Initially 1.87 MW of power is generated and it rises to only 3.9 MW of power which is not equal to plant's rated value. Figures 11 and 12 display active and reactive power.

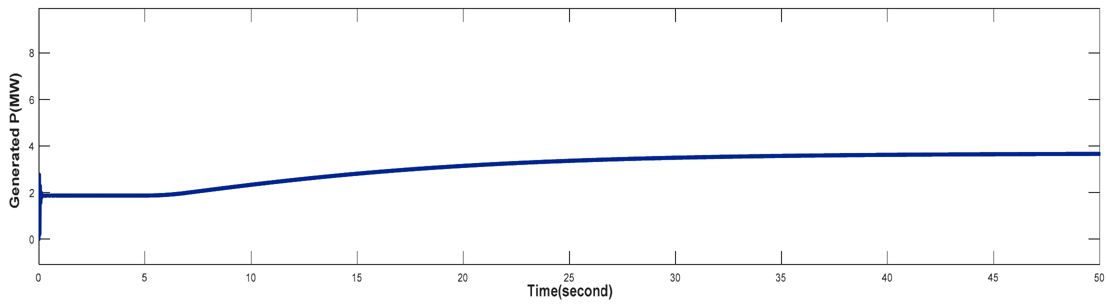

Figure 11. Active power of plant in case of wind speed 8–10 m/s.

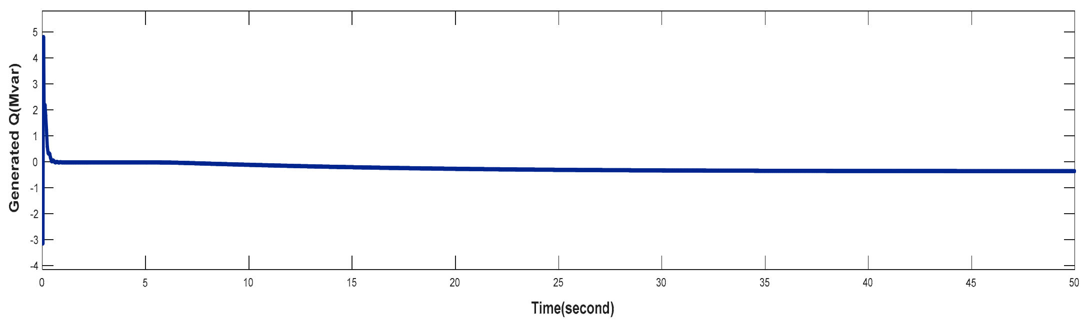

Figure 12. Plant's reactive power when wind speed 8–10 m/s.

Preprints.org (www.preprints.org) | NOT PEER-REVIEWED | Posted: 12 March 2025 doi:10.20944/preprints202503.0844.v1

Figure 13 illustrate that turbine blades' pitch angle is at 0 degree. Pitch angle remains at 0 degree until speed reaches tracking characteristic's point D. Pitch angle is proportionate to speed variation from point D speed after that point. Up to point D, turbine operating point is shown by red curve, as shown in figure 5.

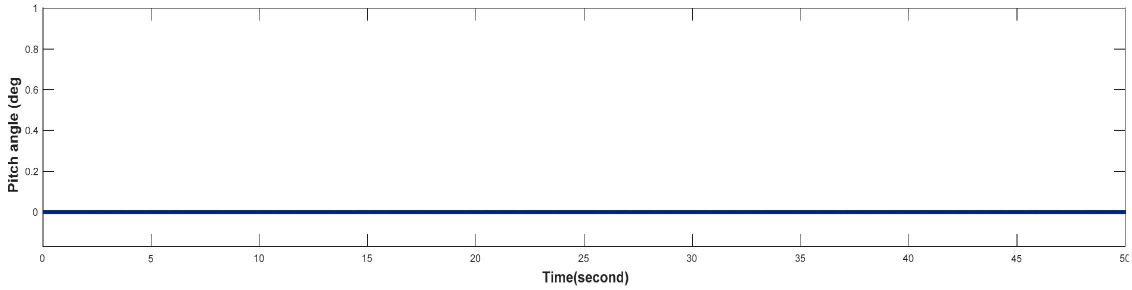

Figure 13. Plant pitch angle in case of wind 8–10 m/s.

4.2. Turbine Response at Rated Value of Wind Speed (Case 2)

Figure 14 shows the wind speed surging from 8 m/s to 14 m/s. As turbine speed increases, active power reaches its nominal value in about 15 seconds, with turbine speed rising to 1.21 pu (21% higher than initially).

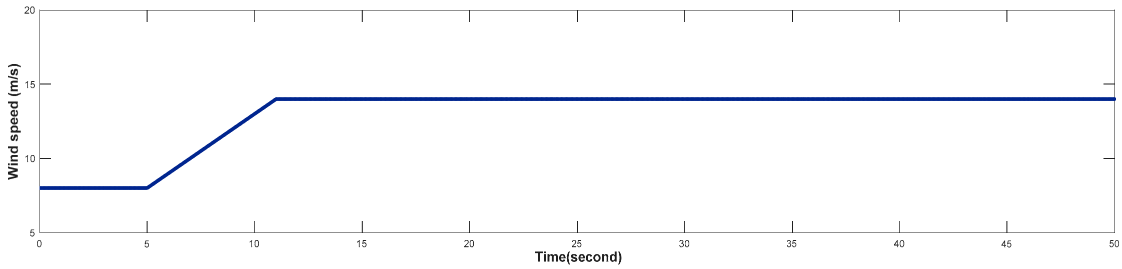

Figure 14. Wind speed changes from 8–14 m/s.

Pitch angle mechanism in wind turbines controls torque and power of turbine rotor, which varies depending on wind speed. The matching regulator output determines pitch angle. This angle is initially zero, and turbine operating point is in accordance with standard turbine characteristic. Pitch angle increases to 0.79 in t=19 sec to prevent turbine's power from increasing further. Amount of generated power, both active and reactive, influenced by this angle. Reactive power is negative and generated active power is limited to 7.3 MW, meaning that reactive power consumed by wind turbines is approximately 0.68 MVAr. It is important to remember that voltage regulation involves turbines. As seen in Figures 15–18, voltage increases upto 1.021pu or 2.1% if mode in VAR control changes.

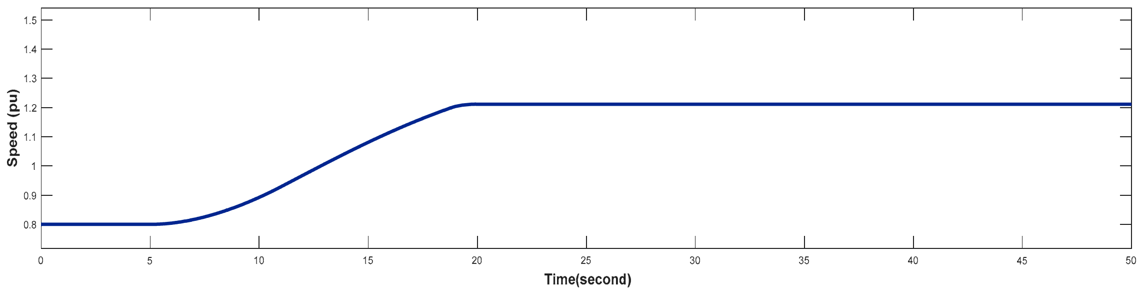

Figure 15. Turbine rotor speed when wind speed changes from 8–14 m/s.

Preprints.org (www.preprints.org) | NOT PEER-REVIEWED | Posted: 12 March 2025 doi:10.20944/preprints202503.0844.v1

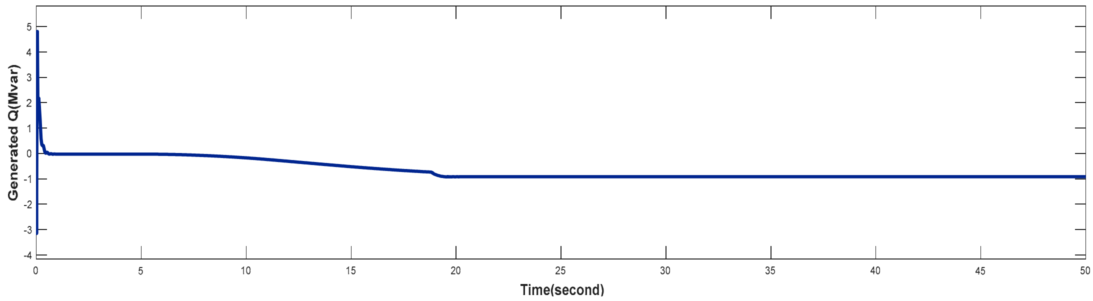

Figure 16. Reactive power of the plant when wind speed changes from 8–14 m/s.

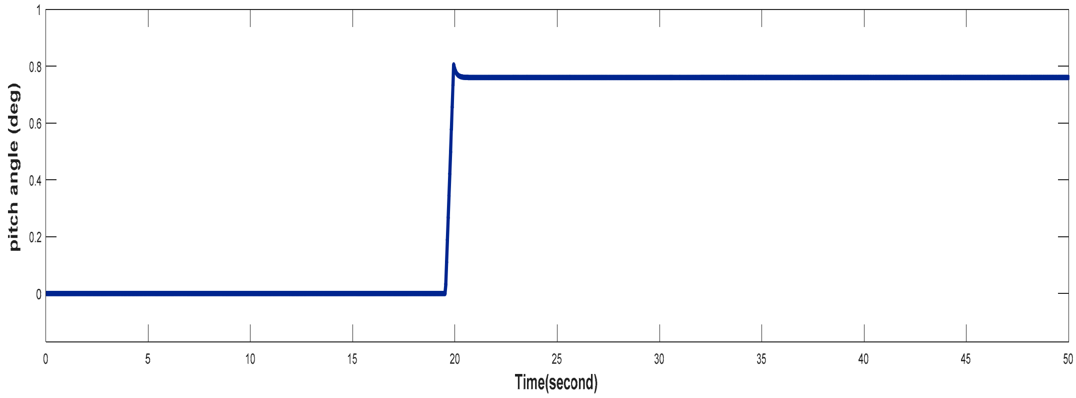

Figure 17. Pitch angle of the plant in the 8–14 m/s wind scenario.

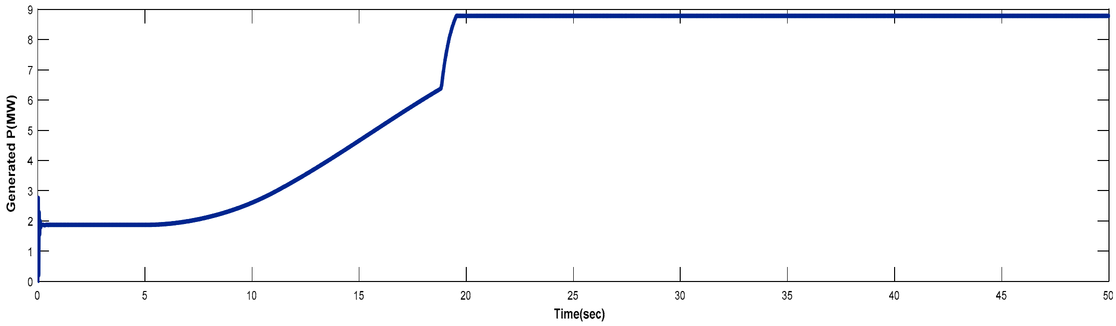

Figure 18. Plant's active power when the wind is blowing between 8 and 14 m/s.

In instances when there is an abrupt shift in wind speed from 8 to 14 m/s while turbine is in voltage regulation mode, variations in turbine speed, reactive power, pitch angle, and active power are displayed in Figures 14, 16, 17, and 18. As can be observed, reactive power starts to fluctuate at about t=19 seconds, while active power rises. However, pitch angle mechanisms begin to respond to limit the turbine's ability to create more active power.

4.3. Turbine Response When Wind Speed Greater Than its Rated Value (Case 3)

To observe the turbine's response while the wind speed varies. Figure 19 illustrate how wind speed increases abruptly to 20 m/s at t = 5 seconds after being initially set at 8 m/s.

Preprints.org (www.preprints.org) | NOT PEER-REVIEWED | Posted: 12 March 2025 doi:10.20944/preprints202503.0844.v1

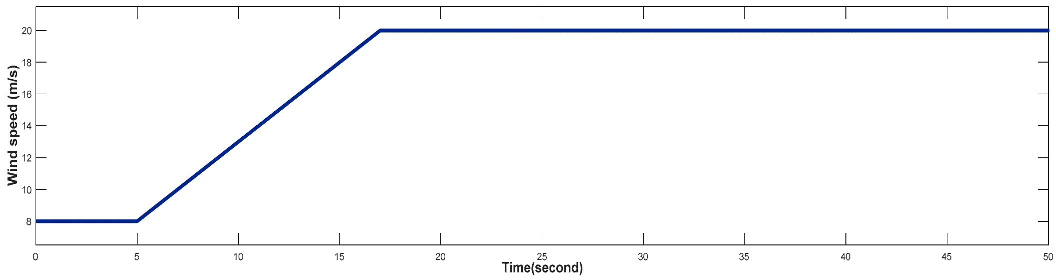

Figure 19. Wind speed changes 8–20m/s.

The rotor speed increases gradually and eventually settle to its rated value of 1.2pu after a few milliseconds when wind speed unexpectedly shifts from 8–20 m/s. Figure 20 depicts the rotor speed (ωr) behavior.

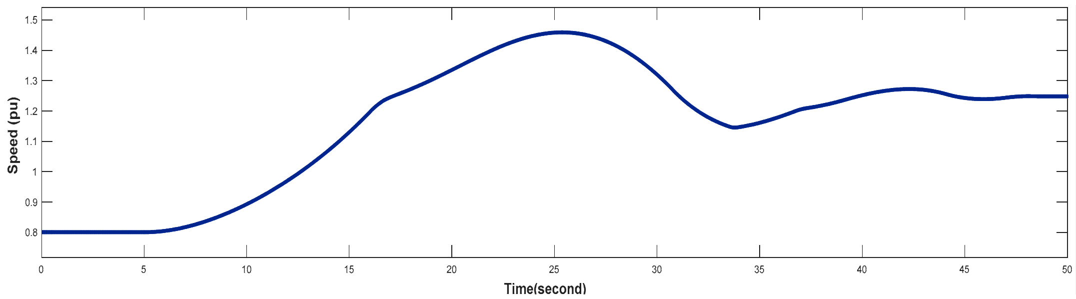

Figure 20. Turbine rotor speed when speed changes 8–20 m/s.

As speed of wind changes, the current changes and thus the power generated changes. Initially 1.87 MW of power is generated and it rises to about 8.8 MW of power and becomes constant for some time until pitch angle variations take place to limit speed of rotor (ωr) shown in Figures 21–23.

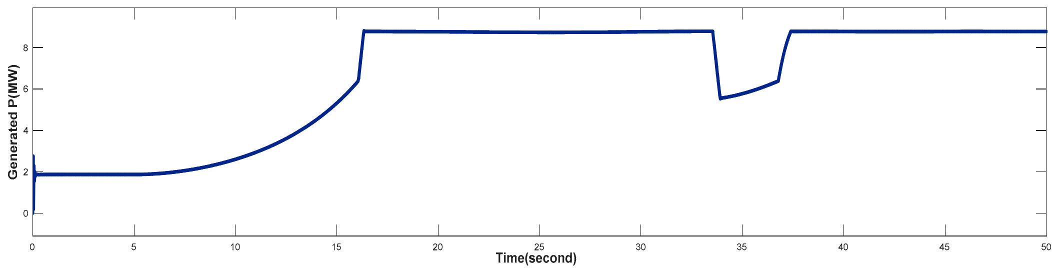

Figure 21. Active power of plant when speed changes from 8–20 m/s.

Reactive power (Q) is absorbed by Wind Farm to maintain voltages at 1pu. Due to variations in farm's power and current, DC link voltage fluctuates with wind speed. Rotor speed varies in response to changes in wind speed. Figures 19 and 20 show that, despite the wind speed fluctuating significantly, the rotor speed varies smoothly, lowering the mechanical strains on the shaft.

Preprints.org (www.preprints.org) | NOT PEER-REVIEWED | Posted: 12 March 2025 doi:10.20944/preprints202503.0844.v1

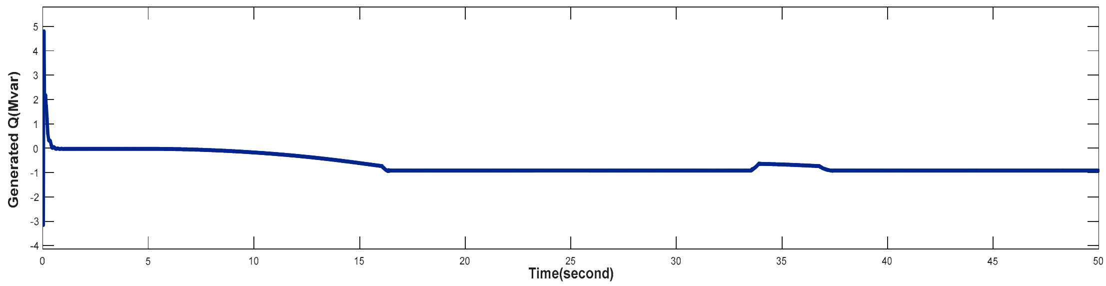

Figure 22. Reactive power of plant when speed changes from 8–20 m/s.

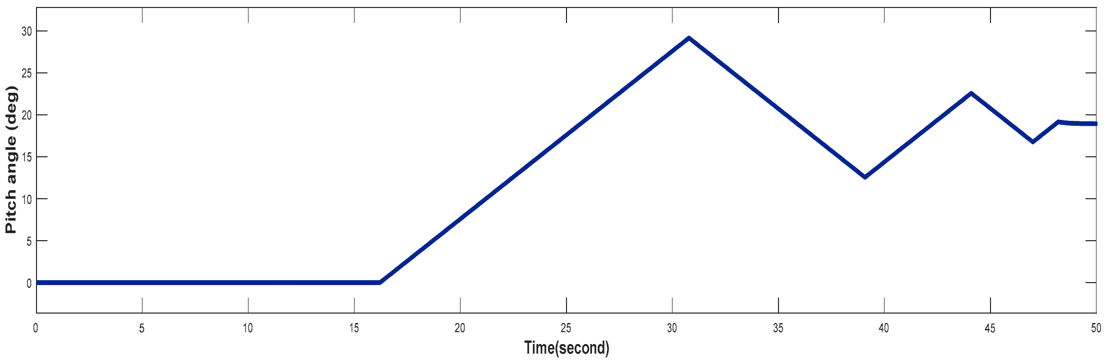

Figure 23. Pitch angle of plant when speed changes from 8–20 m/s.

As soon as speed hits its maximum limit (1.2pu), pitch angle enters the picture to keep rotor speed within safer parameters. This resulted in fluctuations in the electrical power generated.

The DFIG-based wind energy generation system's operation under rated and variable wind speed conditions has been analyzed and studied through simulation in this part. For a longer simulation period and a faster dynamic response to wind speed variations, the average PWM converter model is used. When wind speed is lower than the converter's rating, it aims to maximize power. To prevent mechanical strains at high wind speeds, speed controller allows dynamic variations in generator speed, while converter maintains the output at rated power.

5. Conclusion and Future Work

5.1. Conclusion

For every nation to prosper socioeconomically, energy is essential. Pakistan is still working on projects including renewable energy. But given Pakistan's existing power production and demand disparity as well as its excessive reliance on finite fossil fuel resources, it is imperative that renewable energy sources that can sustain conventional energy sources profitably be implemented on a large scale soon. A brief and thorough overview of wind turbine model utilizing DFIG concepts, as employed by today's wind turbine industry, has been presented in this article. Wind farm (9 MW) with six 1.5 MW wind turbines is represented by system model that has been shown. MATLAB/Simulink software version 2020a has utilized to simulate model. To demonstrate its efficacy, the planned wind farm integrated with Grid and its performance examined for a range of wind speed variation scenarios. The model's results showed that by managing the system of back-to-back converters, maximum extractable output power from changeable wind could be obtained. In addition to shielding the system from severe winds, the pitch angle controller maximizes the power generated by sluggish winds.

5.2. Future work

Following are the recommendations to improve the existing work.

 doi:10.20944/preprints202503.0844.v1

This analysis is done in "Voltage regulation" mode of operation only. It can be further analyzed in "Var Regulation" mode to compare that which mode of operation is more preferable for better efficiency of the plant and for the stability of the load under various system disturbances like Voltage Sag and harmonics.
This article can be improved by applying appropriate control strategies in rotor as well as grid side. Because a wind turbine's control and supervision are automated, advantages including lower operating costs, more worker safety, and higher energy production can be achieved.
Fault analysis can be done on the system to analyze the protection system and system dynamics.

References

1. Chhipa, A.A., et al., *MPPT optimisation techniques and power electronics for renewable energy systems: wind and solar energy systems.* International Journal of Swarm Intelligence, 2022. **7**(2): p. 141-167.
2. Qazi, A., et al., *Towards sustainable energy: a systematic review of renewable energy sources, technologies, and public opinions.* IEEE access, 2019. **7**: p. 63837-63851.
3. Zishan, F., et al., *Allocation of Renewable Energy Resources in Distribution Systems while Considering the Uncertainty of Wind and Solar Resources via the Multi-Objective Salp Swarm Algorithm.* Energies, 2023. **16**(1): p. 474.
4. Sayed, E.T., et al., *Renewable energy and energy storage systems.* 2023. **16**(3): p. 1415.
5. Veerendra Kumar, D.J., et al., *Performance evaluation of 1.1 mw grid-connected solar photovoltaic power plant in louisiana.* Energies, 2022. **15**(9): p. 3420.
6. Himri, Y., et al., *Overview of the Role of Energy Resources in Algeria's Energy Transition.* Energies, 2022. **15**(13): p. 4731.
7. Algarni, S., et al., *Contribution of renewable energy sources to the environmental impacts and economic benefits for sustainable development.* Sustainable Energy Technologies Assessments, 2023. **56**: p. 103098.
8. Prasad, R.M. and M.A. Mulla, *Mathematical modeling and position-sensorless algorithm for stator-side field-oriented control of rotor-tied DFIG in rotor flux reference frame.* IEEE Transactions on Energy Conversion, 2019. **35**(2): p. 631-639.
9. Chhipa, A.A., et al., *Modeling and control strategy of wind energy conversion system with grid-connected doubly-fed induction generator.* Energies, 2022. **15**(18): p. 6694.
10. Wilberforce, T., et al., *Effect of bipolar plate material on proton exchange membrane fuel cell performance.* Energies, 2022. **15**(5): p. 1886.
11. Olabi, A.G., et al., *Prospects of fuel cell combined heat and power systems.* Energies, 2020. **13**(16): p. 4104.
12. Chhipa, A.A., et al., *Role of Power Electronics and Optimization Techniques in Renewable Energy Systems*, in *Intelligent Algorithms for Analysis and Control of Dynamical Systems*. 2020, Springer. p. 167-175.
13. Olabi, A.G., et al., *Selection Guidelines for Wind Energy Technologies.* Energies, 2021. **14**(11): p. 3244.
14. Benbouhenni, H., et al., *Enhancement of the power quality of DFIG-based dual-rotor wind turbine systems using fractional order fuzzy controller.* Expert Systems with Applications, 2023: p. 121695.
15. Rao, K. and K. Rao. *Wind energy: Technical considerations–contents*. in *Wind Energy for Power Generation: Meeting the Challenge of Practical Implementation*. 2019. Springer.
16. Xiahou, K., et al., *Control of DFIG's rotor-side converter with decoupling of current loops using observer-based fractional-order sliding-mode regulators.* IEEE Access, 2019. **7**: p. 163412-163420.
17. Rajendran, M. and L.A. Kumar. *Modeling and Simulation of a DFIG-Based Wind Energy System*. in *Advances in Smart Grid Technology: Select Proceedings of PECCON 2019—Volume I*. 2020. Springer.
18. Nian, H., et al., *Modeling and analysis of DC-link dynamics in DFIG system with an indicator function.* IEEE Access, 2019. **7**: p. 125401-125412.
19. SHAHGHOLIAN, G. and S.M.A. ZANJANI, *A STUDY OF VOLTAGE SAG IN DISTRIBUTION SYSTEM AND EVALUATION OF THE EFFECT OF WIND FARM EQUIPPED WITH DOUBLY-FED INDUCTION GENERATOR.* REVUE ROUMAINE DES SCIENCES TECHNIQUES—SÉRIE ÉLECTROTECHNIQUE ET ÉNERGÉTIQUE, 2023. **68**(3): p. 271-276.
20. Guediri, A., M. Hettiri, and A. Guediri, *Modeling of a wind power system using the genetic algorithm based on a doubly fed induction generator for the supply of power to the electrical grid.* Processes, 2023. **11**(3): p. 952.

doi:10.20944/preprints202503.0844.v1

21. Hore, D. and R. Sarma, *Neural network–based improved active and reactive power control of wind-driven double fed induction generator under varying operating conditions.* Wind Engineering, 2018. **42**(5): p. 381-396.
22. Wang, Z., et al., *Load frequency control of multi-region interconnected power systems with wind power and electric vehicles based on sliding mode control.* Energies, 2021. **14**(8): p. 2288.
23. Eisa, S.A., *Modeling dynamics and control of type-3 DFIG wind turbines: Stability, Q Droop function, control limits and extreme scenarios simulation.* Electric Power Systems Research, 2019. **166**: p. 29-42.
24. Zine, H.K.E. and A. Khoudir, *Design of a High-Performance Control Scheme for a Grid-Connected DFIG-Based Wind Energy Conversion System Using Model Predictive Control and Hysteresis Model.* Elektronika ir Elektrotechnika, 2023. **29**(6): p. 41-49.
25. Singh, P., et al., *Performance Evaluation of Grid-Connected DFIG-Based WECS with Battery Energy Storage System under Wind Alterations Using FOPID Controller for RSC.* Mathematics, 2023. **11**(9): p. 2100.
26. Alami, H.E., et al., *Robust Finite Control-Set Model Predictive Control for Power Quality Enhancement of a Wind System Based on the DFIG Generator*. Energies, 2023. **16**(3): p. 1422.
27. Soomro, M., et al., *Performance improvement of grid-integrated doubly fed induction generator under asymmetrical and symmetrical faults.* Energies, 2023. **16**(8): p. 3350.